Evaluating the Speckle-SFDI for the Quantification of Optical Properties of Biotissues: Modeling and Validation on Optical Phantoms

Boris P. Yakimov[1,2,3], Kirill E. Buiankin[2,3], Anastasia V. Venets[2], and Evgeny A. Shirshin[1,2*]

[1] Laboratory of Clinical Biophotonics, Biomedical Science and Technology Park, Sechenov First Moscow State Medical University, 8 Trubetskaya str., Moscow 119048, Russia

[2] Faculty of Physics, M. V. Lomonosov Moscow State University, 1-2 Leninskie Gory, Moscow 119991, Russia

[3] Moscow State Budgetary Institution of Healthcare "L.A. Vorohobov City Clinical Hospital №67 MHD", 2/44 Salam Adil str., Moscow 123423, Russia

*** e-mail:** shirshin@lid.phys.msu.ru

Abstract. The spatial frequency domain imaging (SFDI) method is rapidly emerging for quantitative mapping of the concentration of tissue chromophores and their scattering coefficients. This method analyzes the optical response of tissues to spatially inhomogeneous radiation with different spatial frequencies, which makes it possible to separate the contributions of absorption and scattering to the diffusely reflected light. However, the projection of spatially inhomogeneous radiation usually requires complex optical schemes, including the use of a spatial light modulator, which is difficult to implement in endoscopes. In this work, we evaluate an alternative approach, in which, instead of analyzing deterministic intensity patterns, the diffuse reflectance at different spatial frequencies can be reconstructed based on the information from random speckle patterns projected onto the surface of the studied tissue, which can be generated without the use of spatial light modulators. We evaluated the speckle-SFDI approach by simulating random speckle patterns and their interaction with turbid and absorptive media with tissue-like optical properties, as well as evaluated this approach experimentally using optical phantoms mimicking properties of real biotissues. The error of absorption and reduced scattering estimation on the number of projected speckles, speckle spatial properties, and optical properties of studied samples was assessed. The suggested approach provided an estimation error of ~10–15% for optical parameters. Given the ease of both experimental and analytical implementation of this technique, it can find applications for quantitative analysis of the optical properties of biological tissues, where "classical" SFDI is hard to implement. The major benefit is the possibility to implement the developed approach within endoscopes.

Keywords: spatial frequency domain imaging; diffuse reflectance spectroscopy; speckles; biophotonics.

Paper #3548 received 7 Oct 2022; revised manuscript received 8 Nov 2022; accepted for publication 25 Nov 2022; published online 18 Dec 2022. doi: 10.18287/JBPE22.08.040509.

1 Introduction

Optical methods are now increasingly used for a wide range of tasks of biomedical diagnostics. Using the optical response, the examined tissue can be characterized in terms of molecular composition or classified as healthy or pathological.

Among the simplest, yet diagnostically valuable optical techniques is diffuse reflectance spectroscopy. Light passing through tissues is partially scattered on inhomogeneities and absorbed by the main tissue chromophores, yielding the reflectance spectra and allowing to perform quantitative composition analysis or classification of a tissue. Diffuse reflectance spectroscopy was demonstrated to be a valuable diagnostic tool in the classification of healthy and cancerous tissues of various organs [1–3], quantification of major tissue chromophores – hemoglobin [4, 5], melanin [6], water, and lipids [7] and less common chromophores, such as carotenoids, bilirubin, etc. [8, 9].

Yet, diffuse reflectance spectroscopy has some disadvantages. Since both scattering and absorption processes contribute simultaneously to the diffuse reflectance, direct quantification of tissues chromophore concentrations requires measuring the diffuse reflectance at different source-detector geometries, e.g., at different distances between the source and detector [10]. Moreover, for most clinical tasks, for example, for intraoperative diagnostics, it is preferable to instantly visualize a macroscopic area of tissues (of the order of several centimeters), which limits the use of fiber probes for diagnostics.

Spatial frequency domain imaging (SFDI) is one of the actively developing extension of the diffuse reflectance spectroscopy that tackles both of the mentioned problems. It allows separating the contributions of scattering and absorption to the diffuse reflectance signal and quantitatively imaging the concentration of chromophores and scattering properties for a macroscopic scanning area. SFDI method is based on the idea that tissue differently reflects spatially-inhomogeneous light of different spatial frequencies – absorption of light significantly influences reflectance at low spatial frequencies, while scattering affects the reflectance at high spatial frequencies. Thus, by projecting spatially inhomogeneous light, for example, intensity, modulated by a sinusoid along one of the spatial coordinates with various spatial frequencies, one can disentangle absorption and scattering contribution to the reflected signal [11, 12]. Signal detection in this case can be performed by a camera, while optical properties (chromophore concentrations and scattering coefficients) can be restored immediately for a macroscopic tissue area. SFDI has been actively used to characterize the severity and depth of burn wounds [13, 14], to assess the concentration of chromophores in healthy and pathological tissues [15, 16] and to classify and characterize them *ex vivo* and *in vivo* [17, 18]. A larger number of SFDI application examples are given in Ref. [19].

The technical disadvantage of the SFDI method is the need to project patterns with different spatial frequencies onto the surface of an investigated object. This, in particular, limits the niche of SFDI in studying tissues of the internal organs *in vivo* with the use of endoscopic systems. Only a limited number of works have demonstrated the possibility of implementing the SFDI method in an endoscopic scheme. In Refs. [20, 21] SFDI was implemented in a rigid endoscope configuration, in which structured illumination (sinusoidal patterns) was transmitted by a separate projection channel of the custom-build endoscope to the tissue surface. In the work [22], an imaging fiber bundle with a large number of fibers was used to transmit structured illumination to the tip of an endoscope in order to use SFDI to quantify the concentration of doxorubicin in tissues. The evaluation of optical properties in the endoscopic scheme is also proposed to be combined with the SFDI Single Shot Optical Properties processing method, which uses only one spatial frequency to determine the absorption and scattering coefficients of tissues [20, 21, 23].

In this paper, we explore an alternative approach that allows the implementation of SFDI in an endoscopic scheme, avoiding the need to transmit structured illumination through the endoscopic optical system using a complex setup. This approach was recently proposed in Refs. [24, 25] and is based on the analysis of the diffuse reflectance obtained from random speckle patterns, which can be generated by the coherent light source and can be transmitted via a simple optical fiber. Speckles have physical properties suitable for this purpose. On the one hand, the speckle pattern is a stationary random process (i.e., its characteristics as a random process do not change in time) [26], on the other hand, it is spatially inhomogeneous, thus allowing analysis of the reflectance at different spatial frequencies. The authors of works [24, 25] suggested to analyze the diffuse reflectance at different spatial frequencies by calculating the spatial autocorrelation function of the detected speckle pattern, from which, according to the Wiener-Khinchin theorem, one can calculate the power spectral density of the intensity at different spatial frequencies and estimate the diffuse reflection at different spatial frequencies and the absorption μ_a and reduced scattering μ'_s coefficients.

Here we demonstrate the possibility of using a simplified algorithm in which the amplitude of the Fourier transform of the captured speckle pattern is used to restore the diffuse reflectance at different spatial frequencies and to estimate absorption and scattering coefficients without the calculations of the spatial autocorrelation function. We describe the algorithm for estimation of absorption and scattering coefficients from the images of the diffusely reflected speckle pattern, evaluate possible sources of errors of the introduced algorithm, and demonstrate the possibility of mapping absorption and scattering coefficients by the proposed procedure experimentally using homogeneous phantoms that mimic optical properties of real biotissues by projecting simulated speckle patterns using custom-build

SFDI setup. We believe this approach can be further adapted for the implementation with optical fibers and used in endoscopic systems for quantitative analysis of tissue optical properties.

2 Materials and Methods

2.1 Speckle Simulation Algorithm

The algorithm used to simulate projected speckle patterns is described in Ref. [26]. Briefly, to imitate free-space propagation and far-field observation speckle intensity maps consisted of n × n pixels, first the (n / k) × (n / k) matrix of random phases uniformly distributed in the [0, 2π] range was generated, where k is the positive integer, which characterizes the "grain" size of the speckle. Second, the complex exponents for the generated phases were calculated to produce so-called random phasors field. Obtained random phasors matrix was then padded with zeros to get the n × n matrix, and after that the array of random phasors was transformed into resulting speckle intensity patterns by the forward Fourier transform (simulating the propagation of waves with random phases into the free space) and by calculation of the absolute value of the Fourier transform amplitude to get intensity of the speckle field.

2.2 Visualization and Data Analysis

Simulation of the projected speckle patterns, interaction of speckle patterns with diffusely reflecting objects, visualization and data analysis were implemented in custom-build Python scripts using NumPy, SciPy, Pandas and Matplotlib modules.

Relative error of the estimated optical parameters was calculated $\delta = \frac{|t-p|}{t}$, where p is the value of the parameter predicted by the algorithm and t is the true value of the parameter. By the intensity at given spatial frequency the amplitude of the Fourier-transformed intensity image at the given spatial frequency is meant.

2.3 Optical Phantoms Fabrication Protocol

To experimentally verify the evaluated speckle-SFDI technique, liquid homogeneous phantoms were used both as reference and test objects, in which a 20% lipofundin solution (Lipofundin MCT/LCT 20%, Braun Melsungen AG, Melsungen, Germany) in water was used as a scatterer, and water-soluble nigrosine (Vektone, Saint Petersburg, Russia) was used as an absorber. The concentrations of scatterer and absorber were selected so that the reduced scattering and absorption coefficients of reference phantom at 630 nm were 20.7 cm^{-1} and 2.01 cm^{-1}, while for test phantom reduced scattering and absorption coefficients were equal to 11.2 cm^{-1} and 3.0 cm^{-1}, respectively. This values of the absorption and reduced scattering coefficients are of the same order of magnitude as the values of absorption and reduced scattering coefficients of skin, its layers and other soft tissues in the 500–700 nm range [27, 28].

2.4 Experimental SFDI Setup

A custom-build experimental setup was used to project synthetic speckle patterns and to detect reflected intensity maps from reference and test phantoms. A commercially available digital micromirror device (DMD)-based projector (TouYinger D021, Everycom Technology, Shenzhen, China) was used to project patterns. The LED light source with emission maxima at 630 nm and full-width at half-maxima of 10 nm was used as a light source. To detect the signal, a monochrome CMOS camera (CS135MUN, Thorlabs Inc., Newton, NJ, USA) was used. The images with 1024 × 1280 pixels were captured using a varifocal objective (20R0001604, Navitar, Rochester, NY, USA).

With the described setup, multiple synthetically generated speckle patterns (generated by the algorithm described in Section 2.1 with n = 1600 and k = 5) were projected onto the surface of the studied phantoms and captured for the subsequent analysis.

3 Results

3.1 Simulation of Speckle Interaction with Turbid Media

To develop and evaluate the algorithm of estimation of tissues absorption and scattering coefficients by the analysis of the reflected speckle patterns, we simulated the free-space speckle patterns and modeled their interaction with the scattering and absorptive homogeneous semi-infinite media. Speckle patterns simulation procedure is described in Materials and Methods (Section 2.1). A typical intensity map of simulated speckle pattern and its 2D Fourier spectrum of amplitudes (i.e. intensity at given spatial frequency) are shown in Fig. 1A.

To model the interaction of a speckle pattern with a diffusely scattering and absorbing media, we used the fact that within the framework of the diffuse approximation of the light transport equation, it can be assumed that each spatial frequency of the incident irradiation independently interacts with the tissue [11, 12]. In the range of scattering an absorption coefficients characteristic for biological tissues in the visible and near infrared range (μ_a ~ 0.01–10 cm^{-1} ≪ μ_s' ~10–100 cm^{-1}) tissue effectively acts as a low-pass filter and significantly affects the attenuation of high spatial frequencies. The dependence of the reflectance *R(k)* on the spatial frequency for a biological tissue with an absorption coefficient μ_a = 1 cm^{-1}, and a scattering coefficient μ_s' = 10 cm^{-1} (anisotropy factor g = 0.9) is shown in Fig. 1B. The formulas describing the dependency of the reflectance on the spatial frequencies are also summarized in Fig. 1B below.

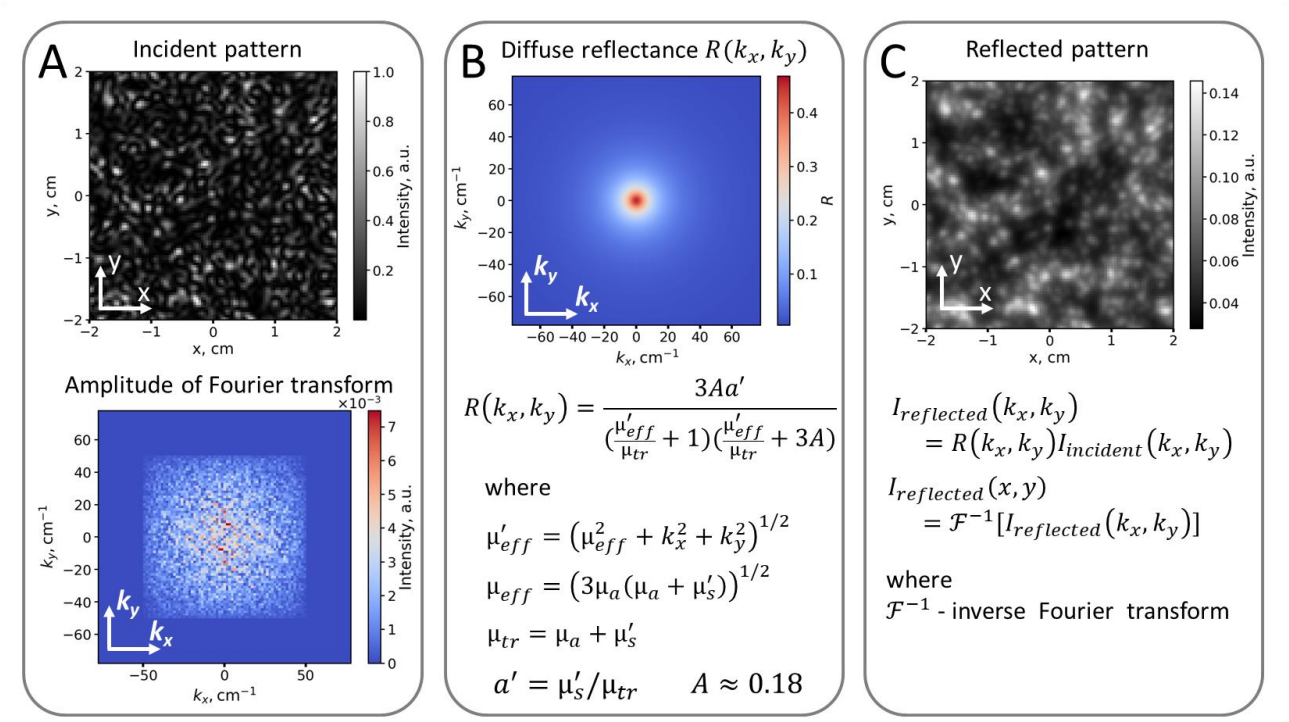

Fig. 1 (A) Intensity map of the simulated speckle and corresponding map of 2D Fourier intensity amplitudes before interaction of the speckle with the scattering medium. (B) Map of the diffuse reflectance coefficient *R* for different spatial frequencies for a semi-infinite medium within the framework of diffuse approximation for media with absorption coefficient $\mu_a = 1$ cm^{-1} and reduced scattering coefficient $\mu'_s = 10$ cm^{-1}. The formulas in the panel summarize the dependence of the diffuse reflectance on spatial frequencies in the diffuse approximation. (C) Intensity map of the speckle pattern diffusely reflected from the media with $\mu_a = 1$ cm^{-1} and $\mu'_s = 10$ cm^{-1}. The formulas in the panel summarize the procedure used for the analysis of intensity of the reflected speckle pattern using diffuse reflectance coefficient and intensity map of the incident speckle-pattern.

Due to the independent transformation of the intensity at any selected spatial frequency upon diffuse reflectance, the intensity of a speckle pattern diffusely reflected from the surface can then be obtained as the inverse Fourier transform of the 2D-Fourier spectrum of the incident radiation multiplied by the diffuse reflectance coefficient at a given spatial frequency. As the scattering media effectively acts as a low-pass filter, this, as expected, leads to blurring of the picture of the incident speckle-pattern (Fig. 1C). The formulas for deriving the diffusely scattered speckle pattern from the Fourier spectrum of the incident speckle and $R(k_x, k_y)$ are summarized in Fig. 1C.

3.2 Algorithm for the Determination of the Absorption and Scattering Coefficients of Tissues from the Properties of Reflected Speckle Patterns

Using the modeling procedures described above, we proposed and tested an algorithm that allows one to determine the absorption and reduced scattering coefficients of tissues by analyzing the properties of speckle patterns detected from the sample. This algorithm is similar to the algorithm proposed in Refs. [24, 25], yet, it has a number of differences, in particular, it does not require the calculation of autocorrelation functions of detected images and operates with the amplitude of Fourier-transformed images directly.

The main steps of the algorithm are summarized in Fig. 2. To measure absorption and scattering properties of the sample with unknown optical properties, a reference phantom with known (μ_a, μ'_s) must be measured first (Fig. 2A). After that, measurements can be performed for the investigated sample (Fig. 2B). At the first step of the algorithm, the speckle pattern is measured for a reference sample (Fig. 2A.1). For the detected image, the Fourier transform of the intensity map is performed and the amplitude of the intensity at each spatial frequency is calculated (Fig. 2A.2). As the Fourier spectrum of the speckle is radially symmetrical, the amplitude of the 2D Fourier spectrum can be radially averaged to reduce the error of the intensity estimation at different spatial frequencies (Fig. 2A.3). Using the estimated values of the intensity of the reflected speckle for different spatial frequencies and the dependence of the diffuse reflectance $R(k_r)$, the dependence of the intensity on the spatial frequency for the incident speckle can be estimated (Fig. 2A.4).

After measuring the reference phantom, similar manipulations have to be performed for the "test" sample. Similarly, to steps (1–3), a scattered speckle pattern is detected for the test sample (Fig. 2B.6), and then a 2D amplitude spectrum of spatial frequencies is calculated for

it, which is averaged radially (Fig. 2B.6). Using the estimated intensity for different spatial frequencies for the investigated test sample and the intensity for the reference phantom, the dependency of the diffuse reflectance on the spatial frequencies $R(k_r)$ can be restored (Figs. 2B.7–8). To estimate the absorption and reduced scattering coefficients from the $R(k_r)$ curve one can fit the curve using analytical formula (Fig. 1B) derived for diffuse approximation or use lookup tables (LUT) obtained via Monte-Carlo simulation of light transport in tissues (Fig. 2B.8). Instead of using diffuse reflectance estimated using diffuse approximation, one can use diffuse reflectance obtained via Monte-Carlo simulation to use at steps (4, 7, 8) of the algorithm.

To use this algorithm for mapping the μ_a, μ_s' values for different regions of tissue, the detected image can be split into individual regions of interest, and steps (1–8) of the algorithm can be performed for them.

3.3 Estimation of the Speckle-SFDI Performance: Model Data

Since the projected speckle patterns are random, the question of the robustness of this technique arises, and how the error of estimation of optical parameters depends on the properties of the projected speckle patterns. We considered three factors that can possibly affect the error of determination of absorption and scattering coefficients using speckle-SFDI.

First, we estimated how the error of optical parameters estimation depends on the number of projected speckle patterns. For this we simulated the work of the algorithm using speckle patterns reflected from the reference object with $\mu_a = 1$ cm^{-1} and $\mu_s' = 10$ cm^{-1} and optical response from the test object with $\mu_a = 0.5$ cm^{-1}, $\mu_s' = 15$ cm^{-1}. The spectrum of intensities at different spatial frequencies was averaged for several separate speckle patterns projected onto a given medium (at steps 1–3 for the reference object and steps 5–6 for the test object), and then the dependence of the diffuse reflectance on the spatial frequency of the test sample was determined using averaged spatial frequency spectra, and the μ_a, μ_s' parameters of the test object were estimated. Fig. 3A shows the dependence of the relative error in determining the absorption and scattering coefficients on the number of speckle patterns used in the simulation. It was found that the relative error decreases proportional to the $N^{-1/2}$ (N – number of speckles), and reaches the level of 5–10% upon averaging over 10 speckles or more. Therefore, further, when varying other speckle parameters, the number of speckle patterns used for the estimation was fixed at 20 in order to exclude errors associated with the random nature of speckles.

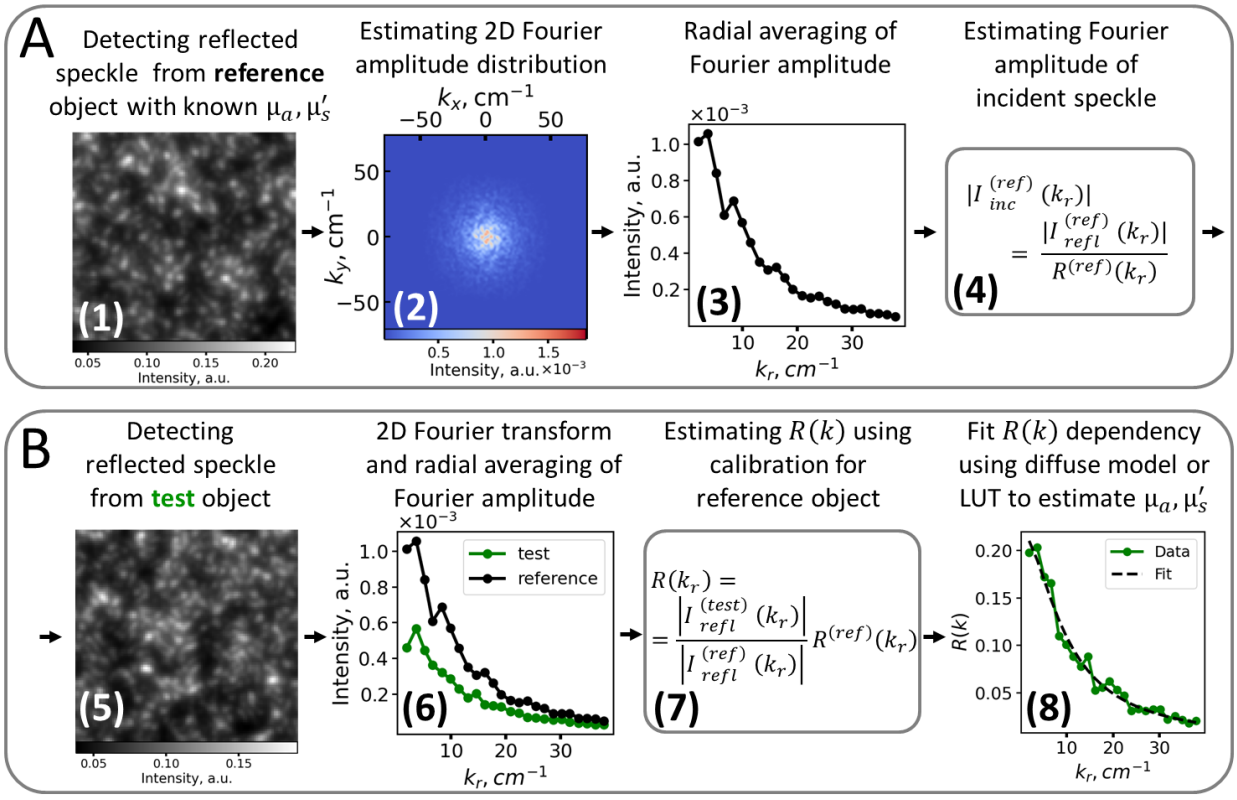

Fig. 2 The main steps of the algorithm for the determination of the absorption and scattering coefficients from the properties of diffusely reflected speckle patterns, carried out with a reference phantom (A) and with the studied (test) object (B). Steps (1–8) are described in the text.

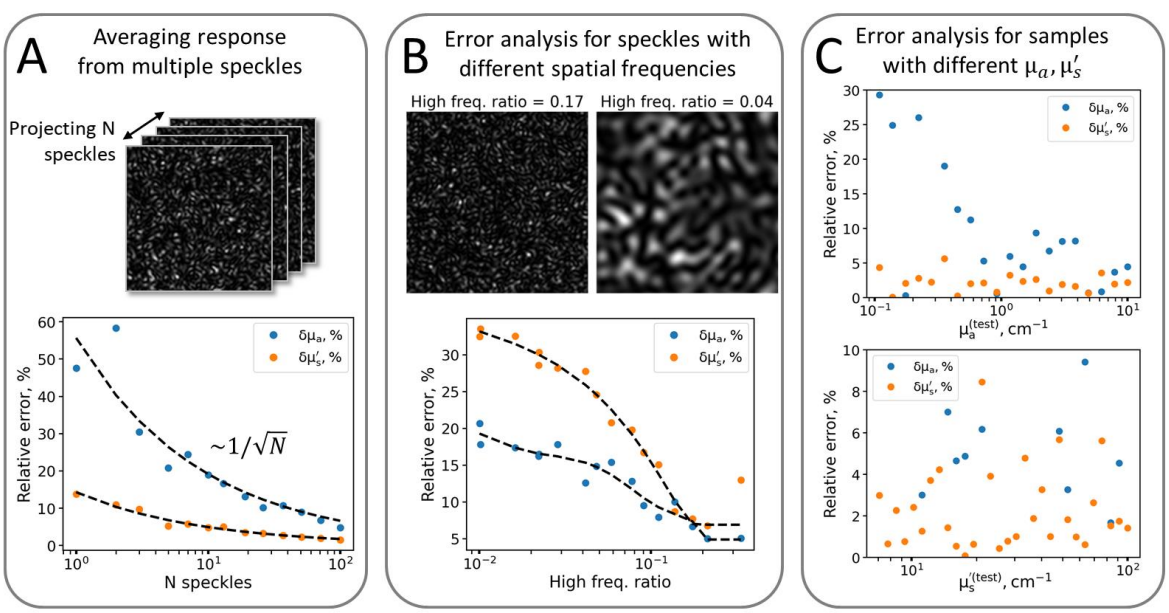

Fig. 3 The dependence of the relative error of the determination of the absorption coefficients μ_a and reduced scattering coefficients μ_s' of the test object (A) on the number of projected speckles, (B) on the size of the spatial inhomogeneity of the speckles estimated as the ratio between average intensity in the (5, 50] cm^{-1} to the average intensity in the (0, 5] cm^{-1} range, (C) on the true values of the absorption and scattering coefficients of the test object.

Another important parameter may be the size of the spatial inhomogeneities of the speckle which are formed upon random interference of the field of coherent light source. We estimated the influence of the inhomogeneity size on the estimation error of the optical parameters of the test samples. Since the speckle pattern has a continuous spatial frequencies spectrum, to characterize the size of the spatial inhomogeneity we introduced the "high spatial frequency ratio" parameter which is calculated as the ratio between the average intensity in the range from (5, 50] cm^{-1} to the average intensity in the range (0, 5] cm^{-1}. The larger this high frequency ratio is, the lower is the size of the observed inhomogeneities. The dependence of the relative error of μ_a, μ_s' estimation on the introduced high spatial frequency ratio is shown in Fig. 3B. As can be seen, at the values of high frequency ratio larger than 0.1, the relative error of μ_a and μ_s' estimations are lower than 10%, and increases significantly upon the decrease of high spatial frequency ratio (i.e., when the size of the spatial inhomogeneity increases) and reaches ~ 35% for the relative error of μ_s' estimation and ~ 20% for the estimation of μ_a when high frequency ratio is equal to 0.01.

Finally, we evaluated the error in determining the parameters of test phantoms with different absorption and scattering coefficients (Fig. 3C). We observed that when the absorption coefficient of the test object varies in the range from 0.1 to 10 cm^{-1}, the error of its determination is about 10%, and increases to 15–30% with a decrease in the absorption coefficient down to 0.1 cm^{-1}, while the error in determining the scattering coefficient is practically unchanged neither in the case of variation in the absorption coefficient, nor in the case of variation in the scattering coefficient of the test phantom in the range from 10^2 to 10^3 cm^{-1} (at the anisotropy factor g = 0.9).

Thus, we see that with the optimal selection of the algorithm parameters – the number of speckles, the size of the speckle inhomogeneities – an error on the order of 5–10% in determination of the optical parameters of the sample can be achieved.

3.4 Experimental Verification of the Absorption and Scattering Speckle-Based Estimation

Next, we evaluated the performance of the proposed algorithm on the real experimental data using the homogeneous phantoms mimicking optical properties of the tissues. For this, we used a phantom based on an aqueous solution of lipofundin acting as a scatterer and nigrosine acting as an absorber.

To generate speckle patterns, we used a custom-made SFDI setup that allows projecting various types of images, including synthetic random speckle patterns with fixed properties. We used speckles with a large contribution of high spatial frequencies to the spatial frequency spectrum. As a reference phantom, we used a phantom with an absorption coefficient of 2 cm^{-1} and a reduced scattering coefficient of 20 cm^{-1} at a wavelength of 630 nm and a phantom with absorption coefficient of 3 cm^{-1} and reduced scattering of 11 cm^{-1} as the test object. These values of the coefficients of absorption and reduced scattering are close to the values of the coefficients of reduced scattering and absorption of the skin, its individual sublayers, as well as other soft tissues in the range of 500–700 nm [27, 28] and were the same orders of magnitude as the values used in modeling in Sections 3.1–3.3.

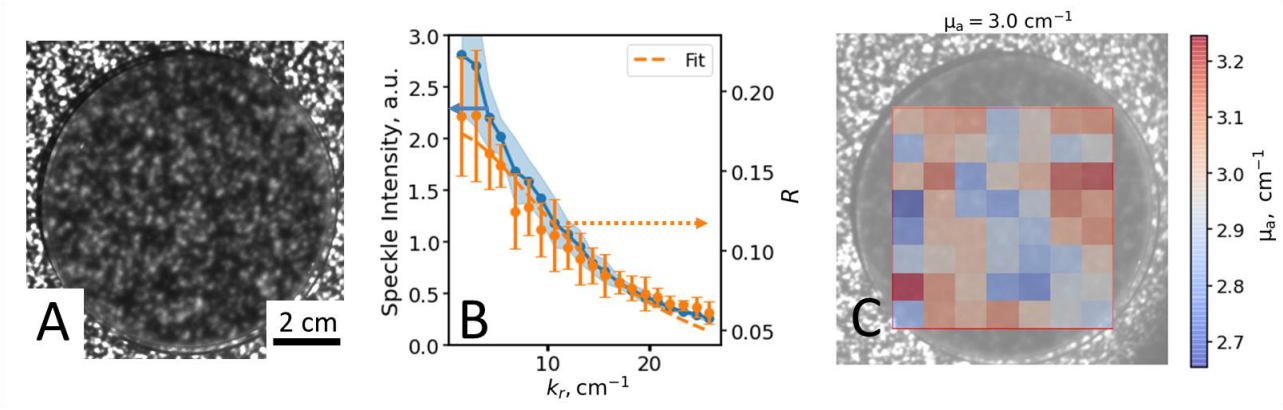

Fig. 4 (A) A typical image of the speckle pattern projected onto an optical phantom. (B) Dependence of the intensity and the diffuse reflectance coefficient on the spatial frequency for the reference phantom. (C) Absorption coefficient map estimated for the test phantom with μ_a = 3 cm^{-1}.

An example of a projected speckle is shown in Fig. 4A. Using the algorithm described in Section 2, we calculated the spatial frequency intensity spectra and estimated the diffuse reflectance dependence on the spatial frequency for the test phantom (Fig. 4B). Finally, by applying the algorithm to ROIs with the size of 1 × 1 cm^2, we verified that for different parts of the image, the absorption coefficient varies in the range from 2.7 to 3.2 cm^{-1}, i.e. the error in determining the absorption coefficient was about 10%.

4 Discussion

In this work we evaluated the method of determination of the absorption and reduced scattering coefficients of the diffusely reflecting samples, e.g. biotissues, that involves the analysis of the spatial frequency spectrum of random speckle patterns projected onto the surface of the sample. This method is an alternative approach to the "classical" SFDI technique, which maps the absorption and scattering coefficients of object by analyzing its optical response to the spatially inhomogeneous intensity patterns (usually modulated by sinusoid) with different spatial frequencies varied from 0 up to 20 cm^{-1}.

The speckle-SFDI method initially proposed in Ref. [24, 25] and evaluated in this work uses random speckle patterns as inhomogeneous intensity field instead of deterministic sinusoidal intensity patterns. The benefit of this approach is in the lack of necessity to use spatial light modulators and complex optical schemes to transmit structured illumination to the surface of the sample, for example, in an endoscopic scheme – speckles can be generated using coherent light sources and can be formed after leaving the optical fibers directly [26], while the optical fiber can be easily combined with standard endoscopes. Although the optical and statistical properties of speckle patterns generated by multimode fibers differ globally from the properties of "free-space" speckle patterns, they are locally similar [29], thus the obtained results should be valid for both types of speckles.

In this work we modified the algorithm for determination of the absorption and scattering coefficients from the properties of speckle patterns proposed in Refs. [24, 25], eliminating the need to calculated the autocorrelation function of the image and directly determining the dependence of the diffuse reflectance on the spatial frequency from radially averaged intensity amplitudes at different spatial frequencies obtained from the Fourier transform of detected speckle (Fig. 2). We evaluated the main sources influencing the determination of absorption and scattering coefficients. In particular, we found that the optical parameters' estimation error decreases as the inverse root of the number of speckle patterns used for averaging (Fig. 3A). This observation can be explained by the fact that speckle patterns over which the averaging is carried out are independent, thus, the accuracy of the estimations obeys the central limit theorem for random values. In the case of averaging the results over incompletely independent speckle patterns, a slower decrease in the error in determining absorption and scattering can be expected.

We also noted that upon reducing the contribution of high spatial frequencies (in the range (5, 50] cm^{-1}) to the spatial frequencies spectrum of random speckles a significant increase is observed for the error of determination of reduced scattering coefficient (up to 35% or even higher), while the error of absorption coefficient increases not so dramatically and remains below the level of 20% (Fig. 3B). This observation can be explained by the fact that the absorption process mainly affects the values of the diffuse reflectance at low spatial frequencies, while scattering affects diffuse reflectance at high spatial frequencies, therefore, with an increase in the size of the spatial inhomogeneity (decrease in the "High frequency ratio" parameter), the largest increase is observed for the error in determining the scattering coefficient. The observed changes in the error of μ_a estimation can be indirectly related to the errors of estimation of μ_s', since both of the parameters are estimated simultaneously.

At the same time, we found that the relative error in determining the scattering coefficients does not change significantly for scattering coefficients varying in the range from 10^2 cm^{-1} to 10^3 cm^{-1} (reduced scattering in 10^1–10^2 cm^{-1}) and is less than 10%. At the same time, the relative error in determining the absorption coefficients

can be about 20–30% in the case of low absorption coefficients (less than 1.0 cm^{-1}). This fact should be taken into account when analyzing the optical properties of tissues in the red and near infrared regions of the spectrum in the so called "transparency window" of biological tissues, where the absorption coefficient of tissues is significantly lower than the blue-green region of the spectrum, where the absorption of hemoglobin and other chromophores predominates [27].

Despite these shortcomings, we believe this approach can be a promising and simple alternative to the "classical" SFDI method and can be easily implemented for endoscopic applications and quantitative analysis of tissue composition, including *in vivo* applications.

5 Conclusion

Here we evaluated a method of estimation of the absorption and reduced scattering coefficients of turbid media such similar to optical properties of biotissues by the analysis of the spatial frequency spectrum of random speckles. The proposed method uses information on the distribution of speckle intensity over different spatial frequencies to determine the dependence of the diffuse reflectance coefficient on the spatial frequency, which can then be fitted to estimate absorption and reduced scattering coefficients of the studied object. Using simulation of random speckles and calculation of their interaction with diffuse-scattering and absorbing media, we estimated the error in determining the absorption and scattering coefficients using the proposed approach and its dependence on the number and parameters of projected speckle patterns, as well as on the optical properties of test objects. An experimental evaluation of the efficiency of the method on homogeneous optical phantoms simulating the properties of tissue was carried out.

The results show that this approach, with the optimal selection of parameters, can be an easy-implemented alternative to the "classical" SFDI method and can be used to estimate the absorption and scattering coefficients of media with an accuracy of about 10–15%, in particular, it can find its niche in the application of SFDI within endoscopic schemes.

Disclosures

Authors declare no competing interests.

Funding

The work was supported by the Russian Science Foundation (grant No. 22-25-00759).

Acknowledgement

This research was performed according to the Development Program of the Interdisciplinary Scientific and Educational Schools of Lomonosov Moscow State University "Photonic and Quantum Technologies. Digital medicine" and according to the Academic leadership program Priority 2030 proposed by Federal State Autonomous Educational Institution of Higher Education I.M. Sechenov First Moscow State Medical University of the Ministry of Health of the Russian Federation (Sechenov University).

References

1. Z. I. Volynskaya, A. S. Haka, K. L. Bechtel, M. D. Fitzmaurice, R. Shenk, N. Wang, J. Nazemi, R. R. Dasari, and M. S. Feld, "Diagnosing breast cancer using diffuse reflectance spectroscopy and intrinsic fluorescence spectroscopy," Journal of Biomedical Optics 13(2), 024012 (2008).
2. Z. Ge, K. T. Schomacker, and N. S. Nishioka, "Identification of Colonic Dysplasia and Neoplasia by Diffuse Reflectance Spectroscopy and Pattern Recognition Techniques," Applied Spectroscopy 52(6), 833–839 (1998).
3. M. S. Nogueira, S. Maryam, M. Amissah, H. Lu, N. Lynch, S. Killeen, M. O'Riordain, and S. Andersson-Engels, "Evaluation of wavelength ranges and tissue depth probed by diffuse reflectance spectroscopy for colorectal cancer detection," Scientific Reports 11(1), 798 (2021).
4. J. E. Bender, A. B. Shang, E. W. Moretti, B. Yu, L. M. Richards, and N. Ramanujam, "Noninvasive monitoring of tissue hemoglobin using UV-VIS diffuse reflectance spectroscopy: a pilot study," Optics Express 17(26), 23396–23409 (2009).
5. L. Dolotov, Y. P. Sinichkin, V. Tuchin, S. Utz, G. Altshuler, and I. Yaroslavsky, "Design and evaluation of a novel portable erythema-melanin-meter," Lasers in Surgery and Medicine 34(2), 127–135 (2004).
6. D. Yudovsky, L. Pilon, "Rapid and accurate estimation of blood saturation, melanin content, and epidermis thickness from spectral diffuse reflectance," Applied Optics 49(10), 1707–1719 (2010).
7. G. S. Budylin, D. A. Davydov, N. V. Zlobina, A. V. Baev, V. G. Artyushenko, B. P. Yakimov, and E. A. Shirshin, "In vivo sensing of cutaneous edema: A comparative study of diffuse reflectance, Raman spectroscopy and multispectral imaging," Journal of Biophotonics 15(1), e202100268 (2022).
8. M. E. Darvin, C. Sandhagen, W. Koecher, W. Sterry, J. Lademann, and M. C. Meinke, "Comparison of two methods for noninvasive determination of carotenoids in human and animal skin: Raman spectroscopy versus reflection spectroscopy," Journal of Biophotonics 5(7), 550–558 (2012).
9. S. K. Alla, A. Huddle, J. D. Butler, P. S. Bowman, J. F. Clark, and F. R. Beyette, "Point-of-Care Device for Quantification of Bilirubin in Skin Tissue," IEEE Transactions on Biomedical Engineering 58(3), 777–780 (2011).

10. A. Kienle, L. Lilge, M. S. Patterson, R. Hibst, R. Steiner, and B. C. Wilson, "Spatially resolved absolute diffuse reflectance measurements fornoninvasive determination of the optical scattering and absorption coefficientsof biological tissue," Applied Optics 35(13), 2304–2314 (1996).
11. D. J. Cuccia, F. Bevilacqua, A. J. Durkin, and B. J. Tromberg, "Modulated imaging: quantitative analysis and tomography of turbid media in the spatial-frequency domain," Optics Letters 30(11), 1354–1356 (2005).
12. D. J. Cuccia, F. P. Bevilacqua, A. J. Durkin, F. R. Ayers, and B. J. Tromberg, "Quantitation and mapping of tissue optical properties using modulated imaging," Journal of Biomedical Optics 14(2), 024012 (2009).
13. A. Ponticorvo, D. M. Burmeister, B. Yang, B. Choi, R. J. Christy, and A. J. Durkin, "Quantitative assessment of graded burn wounds in a porcine model using spatial frequency domain imaging (SFDI) and laser speckle imaging (LSI)," Biomedical Optics Express 5(10), 3467–3481 (2014).
14. D. M. Burmeister, A. Ponticorvo, B. Yang, S. C. Becerra, B. Choi, A. J. Durkin, and R. J. Christy, "Utility of spatial frequency domain imaging (SFDI) and laser speckle imaging (LSI) to non-invasively diagnose burn depth in a porcine model," Burns 41(6), 1242–1252 (2015).
15. A. M. Laughney, V. Krishnaswamy, T. B. Rice, D. J. Cuccia, R. J. Barth, B. J. Tromberg, K. D. Paulsen, B. W. Pogue, and W. A. Wells, "System analysis of spatial frequency domain imaging for quantitative mapping of surgically resected breast tissues," Journal of Biomedical Optics 18(3), 036012 (2013).
16. Y. Zhao, Y. Deng, S. Yue, M. Wang, B. Song, and Y. Fan, "Direct mapping from diffuse reflectance to chromophore concentrations in multi-fx spatial frequency domain imaging (SFDI) with a deep residual network (DRN)," Biomedical Optics Express 12(1), 433–443 (2021).
17. S. Tabassum, Y. Zhao, R. Istfan, J. Wu, D. J. Waxman, and D. Roblyer, "Feasibility of spatial frequency domain imaging (SFDI) for optically characterizing a preclinical oncology model," Biomedical Optics Express 7(10), 4154–4170 (2016).
18. Y. Zhao, S. Tabassum, S. Piracha, M. S. Nandhu, M. Viapiano, and D. Roblyer, "Angle correction for small animal tumor imaging with spatial frequency domain imaging (SFDI)," Biomedical Optics Express 7(6), 2373–2384 (2016).
19. S. Gioux, A. Mazhar, and D. J. Cuccia, "Spatial frequency domain imaging in 2019: principles, applications, and perspectives," Journal of Biomedical Optics 24(7), 071613 (2019).
20. J. Angelo, M. Giessen, and S. Gioux, "Real-time endoscopic optical properties imaging using Single Snapshot of Optical Properties (SSOP) imaging," Proceedings of SPIE 9313, 93130P (2015).
21. J. P. Angelo, M. Giessen, and S. Gioux, "Real-time endoscopic optical properties imaging," Biomedical Optics Express 8(11), 5113–5126 (2017).
22. J. Kress, D. J. Rohrbach, K. A. Carter, D. Luo, C. Poon, S. Aygun-Sunar, S. Shao, S. Lele, J. F. Lovell, and U. Sunar, "A dual-channel endoscope for quantitative imaging, monitoring, and triggering of doxorubicin release from liposomes in living mice," Scientific Reports 7(1), 15578 (2017).
23. L. Baratelli, E. Aguénounon, M. Flury, and S. Gioux, "Real-Time, Wide-Field Endoscopic Quantitative Imaging Based on 3D Profile Corrected Deep-Learning SSOP," In European Conference on Biomedical Optics, 20–24 June 2021, Munich, Germany, EM2C.5 (2021).
24. M. T. Chen, M. Papadakis, and N. J. Durr, "Speckle illumination SFDI for projector-free optical property mapping," Optics Letters 46(3), 673–676 (2021).
25. M. T. Chen, T. L. Bobrow, and N. J. Durr, "Towards SFDI endoscopy with structured illumination from randomized speckle patterns," Proceedings of SPIE 11631, 116310Y (2021).
26. J. W. Goodman, "Speckle phenomena in optics: theory and applications," Roberts and Company Publishers, Greenwood Village, CO, United States (2007). ISBN: 9780974707792.
27. A. N. Bashkatov, E. A. Genina, and V. V. Tuchin, "Optical properties of skin, subcutaneous, and muscle tissues: a review," Journal of Innovative Optical Health Sciences 4(01), 9–38 (2011).
28. S. L. Jacques, "Optical properties of biological tissues: a review," Physics in Medicine & Biology 58(11), R37 (2013).
29. N. Takai, T. Asakura, "Statistical properties of laser speckles produced under illumination from a multimode optical fiber," Journal of the Optical Society of America 2(8), 1282–1290 (1985).